



Effect of ephemeral snow cover on the active layer thermal regime and thickness on CALM-S JGM site, James Ross Island, eastern Antarctic Peninsula

Filip Hrbáček^{1*}, Zbyněk Engel², Michaela Kňázková¹, Jana Smolíková^{1,2}

5 ¹ Department of Geography, Faculty of Science, Masaryk University, Brno, Czech Republic

² Department of Physical Geography and Geoecology, Faculty of Science, Charles University, Prague, Czech Republic

Correspondence to: Filip Hrbáček (hrbacekfilip@gmail.com)

Abstract. This study aims to assess the role of ephemeral snow cover on ground thermal regime and active layer thickness in two ground temperature measurement profiles on the Circumpolar Active Layer Monitoring Network – South (CALM-S) JGM site on James Ross Island, eastern Antarctic Peninsula during the high austral summer 2018. The snowstorm of 13–14 January created a snowpack of recorded depth of up to 38 cm. The snowpack remained on the study site for 12 days in total and covered 46% of its area six days after the snowfall. It directly affected ground thermal regime in a study profile AWS-JGM while the AWS-CALM profile was snow-free. The thermal insulation effect of snow cover led to a decrease of mean summer ground temperatures on AWS-JGM by ca 0.5–0.7 °C. Summer thawing degree days at a depth of 5 cm decreased by ca 10% and active layer was ca 5–10 cm thinner when compared to previous snow-free summer seasons. Surveying by ground penetrating radar revealed a general active layer thinning of up to 20% in those parts of the CALM-S which were covered by snow of > 20 cm depth for at least six days.

1. Introduction

Seasonal occurrence of snow cover, its thickness and spatial distribution significantly affect ground thermal regime as well as active layer refreezing in regions underlain by permafrost. It is estimated that a snow accumulation about 40 cm deep has the maximum insulating effect (e.g., Zhang, 2005). Generally, thinner snow accumulation tends to have a cooling effect on the ground while a thicker and long-lasting snow cover can increase the ground temperature. The insulating effect of snow cover in permafrost conditions is the most prominent in winter due to maximum snow thickness, high surface albedo and the porosity of snow, and a large temperature difference between the atmosphere and the ground surface (Callaghan *et al.*, 2011). Under these conditions, the solar energy absorbed by the snow surface is reduced, thermal conduction within the snowpack is low, and the transfer of heat between the air and the soil surface is limited. The net influence of snow over the cold period amounts to an increase of mean ground temperatures and maximum thaw depths, but these effects vary greatly in space and time (Zhang, 2005). At the end of winter the insulating effect of snow decreases, and meltwater becomes the primary influence.



30 During the summer period, the effect of snow on ground temperature and thaw depth is considered to be relatively small under
permafrost conditions (Goodrich, 1982). The ground remains frozen underneath long-lasting snow patches but warms rapidly
in snow-free areas (Harris and Corte, 1992). The infiltration of meltwater increases the thermal conductivity of the ground,
enhancing heat transfer from the ground surface to the permafrost table (Campbell *et al.*, 1998). When ephemeral snow cover
builds up during the summer, snow protects the ground from warm air and the active layer may eventually refreeze from the
permafrost table upwards. However, this cooling effect is limited and its impact on the ground is controlled primarily by the
35 duration of the snow cover, snow properties and a temperature difference between the air and the ground surface. The insulating
capacity of snow increases in late summer when the thaw plane tends to rise rapidly (Goodrich, 1982).

The snow cover effect on ground thermal regime or active layer thawing has been widely studied in the Arctic regions during
the past decades (e.g., Zhang, 2005; Callahan *et al.*, 2011; Johansson *et al.*, 2013; Park *et al.*, 2015). In contrast, the knowledge
on snow-ground interactions in Antarctica is limited mostly to sites within the Antarctic Peninsula region (AP) with only a
40 few studies from different parts of the continent. Generally, snowpack controls the ground thermal regime and active layer
thickness in Antarctica in different ways depending on its seasonal duration and prevailing depth. Only a negligible effect of
winter snowpack on ground thermal regime was observed in dry and cold conditions of the north-eastern AP where snow cover
in winter is irregular and usually thinner than 30 cm (Hrbáček *et al.*, 2016). A ground temperature increase was observed in
cases when snow persists for the majority of the winter with a thickness between 30 and 70 cm. Such conditions are
45 characteristic for the study sites on the South Shetlands in the north-western AP (Oliva *et al.*, 2017a; de Pablo *et al.*, 2017;
Ramos *et al.*, 2017) and they were also observed in topographically similar sites on James Ross Island (Kňázková *et al.*, 2020).
Importantly, ground warming during the thaw season can lead to permafrost degradation especially in areas on the border
conditions between continuous and discontinuous permafrost of the north-western AP (Hrbáček *et al.*, 2020).

At the same time, however, persistent snowpack can lead to active layer thinning and its effect can eventually promote
50 permafrost aggradation. The main reason is a shortening of the thawing season (Ramos *et al.*, 2017). Consequently, the heat
deficit reduces active layer thawing propagation. Such conditions were observed on the South Shetlands after 2010 (de Pablo
et al., 2017; Ramos *et al.*, 2017) and they were related to a recent climate cooling (Turner *et al.*, 2016; Oliva *et al.*, 2017b) and
an associated increase in snow precipitation within the AP region (Carrasco and Cordero, 2020). Similar effect of long-lasting
snow cover was reported from the Victoria Land where the presence of snow prevented the active layer from thawing in the
55 summer completely (Guglielmin *et al.*, 2014a). General cooling of the active layer and permafrost was further observed in
areas where snowpack exceeded 1 m, as reported by Guglielmin *et al.* (2014b) from Adelaide Island. According to Ramos *et al.*
(2020), permanent accumulation of > 4.5 m can even lead to a complete insulation of the ground from atmosphere, causing
permafrost aggradation and forming a specific subnival thermal regime of the ground.

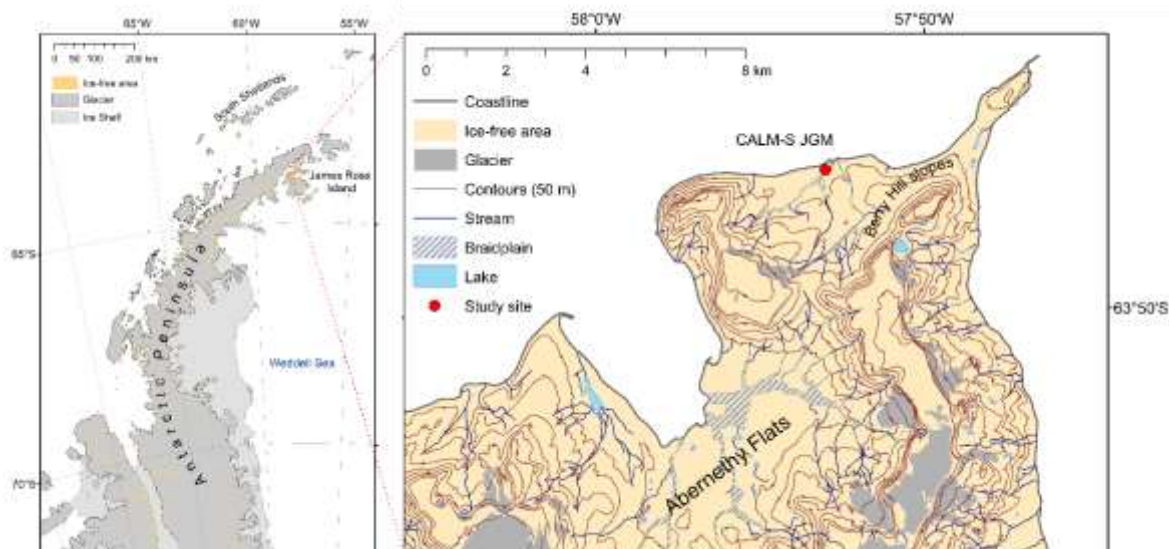
This study brings a new perspective on the effect of snow on ground thermal regime and active layer thickness. We assess the
60 role of a relatively thick ephemeral snowpack that occurred in the high summer 2018 on the area of Circumpolar Active Layer
Monitoring site (CALM-S) JGM on James Ross Island. The objectives of this study are to (i) describe the spatial variability
of snow cover thickness in the study area in January 2018, (ii) assess the differences in ground thermal regime and active layer



thickness between the snow-covered and snow-free sites, and (iii) determine the effect of ephemeral snowpack on active layer thaw depth.

65 2. Study area

James Ross Island is located in the north-eastern sector of the AP (Fig. 1). The northern part of James Ross Island, Ulu Peninsula, constitutes the largest ice-free area in the entire AP. The mean annual air temperature in the lowland parts of JRI (<50 m asl) was $-7.0\text{ }^{\circ}\text{C}$ in the period 2006–2015 with a positive trend of annual temperatures but a cooling trend in the summer (DJF) months (Hrbáček and Uxa, 2020). The annual precipitation is estimated to about 300–700 mm w.e.y⁻¹ (van Wessem *et al.*, 2016, Palerme *et al.*, 2017). Snow cover is distributed irregularly as indicated by perennial snowfields on lee-slopes and snow patches around topographic obstacles. Snow thickness in the flat lowland areas is usually less than 20 cm, but can rarely exceed 40 cm (Hrbáček *et al.*, 2016, Kňazková *et al.*, 2020). The ice-free area is underlain by continuous permafrost with a modelled temperature between $-4\text{ }^{\circ}\text{C}$ and $-8\text{ }^{\circ}\text{C}$ (Obu *et al.*, 2020). The active layer thickness strongly depends on lithology and varies between 50 and 120 cm (Hrbáček *et al.*, 2019).

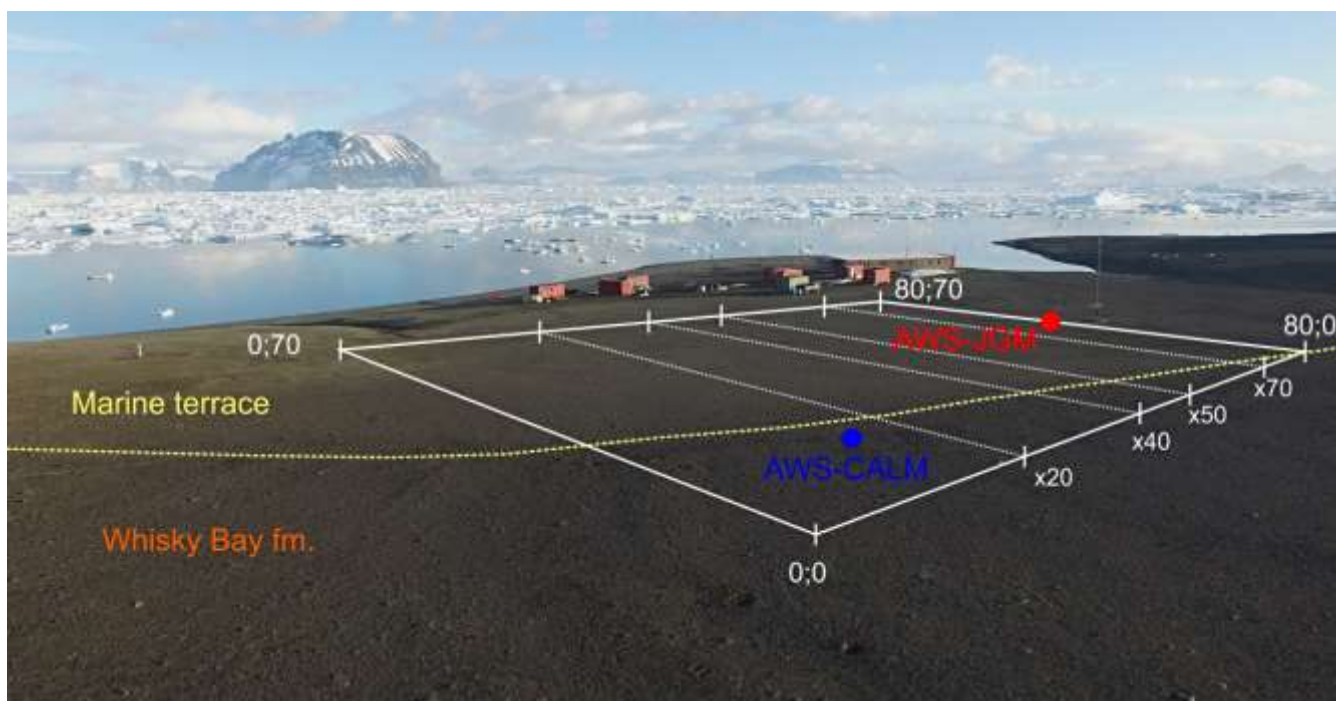


75 **Figure 1 Regional setting (left) and the location of CALM-S JGM site (right)**

The study site is located on the CALM-S JGM which is the part of a continental database (REF). The area of 80 m by 70 m was established in February 2014 following recommendations for CALM-S sites proposed by Guglielmin (2006). The area 80 comprises diverse geological units, with a Holocene marine terrace covering ca 80% of the northern part of the site and Cretaceous Whisky Bay Fm. forming the remaining 20% of the site (Fig. 2). The geological conditions lead to a variability of



general ground physical characteristics and consequently drive the variability of active layer thaw depth which is about 20 cm thicker in the southern part underlain by the Cretaceous sediments (Hrbáček *et al.*, 2017).



85 **Figure 2 Study site from the south-east. The white polygon with local coordinates (x;y) in the corners delimits the area of CALM-S JGM, white dotted lines indicate selected ground penetrating radar profiles shown in Fig. 7, and the yellow dotted line represents the boundary between the geological formations of Holocene marine terrace and Cretaceous Whisky Bay Fm. Colour points represent positions of ground temperature monitoring profiles.**

3. Material and Methods

90 3.1 Temperature monitoring and data processing

There are two automatic weather stations (AWS) installed within the CALM-S JGM grid. The fully equipped site AWS-JGM is located in the part formed by the marine terrace. It provides data on air temperature at 2 m above ground measured by Pt100/8 sensor (accuracy ± 0.15 °C) placed in a radiation shield, and ground temperature measured by Pt100/8 thermometers (accuracy ± 0.15 °C) placed directly in the ground. The second automatic weather station (AWS-CALM) is installed in the
95 Cretaceous sediments about 60 m to the west from AWS-JGM and provides data on ground temperature only. The measurement is conducted by the same thermistors and placed at the same depths as on AWS-JGM. Missing data in the AWS-CALM record in the period 18 December 2016 to 20 January 2017 were replaced using a multiple regression according to air and ground temperature data from AWS-JGM. With regards to the size of the CALM-S JGM area, the air temperatures from AWS-JGM site are considered to be representative also for AWS-CALM (Hrbáček *et al.*, 2017).

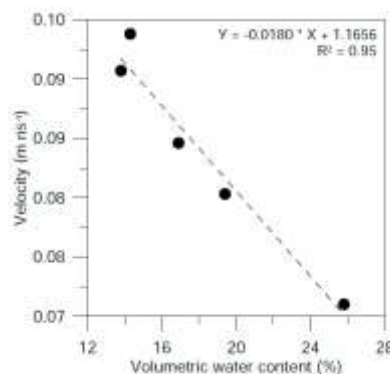


- 100 Climate data were analysed for the austral summer periods 2016/17 and 2017/18. Particularly, the following parameters were calculated:
- a) Daily and seasonal mean air and ground temperatures at depths of 5, 50 and 75 cm;
 - b) Thawing degree days of air and (TDD_A) ground at a depth of 5 cm (TDD₅) calculated as a sum of positive daily temperatures;
 - 105 c) Isothermal days at a depth of 5 cm set as an event with the maximum and minimum daily temperatures within the interval 0.5 °C to -0.5 °C (Guglielmin, 2006).

The daily variability of active layer thaw depth is defined as a maximum daily depth of 0 °C isotherm for the entire period of thawing season and the maximum seasonal active layer thickness is calculated accordingly.

3.2 ALT measurements

- 110 Mechanical probing and ground penetrating radar (GPR) soundings were used to determine seasonal changes of active layer thickness. Thaw depths were measured on 31 January and 12 February during the summer period 2016/17 and on 20 January, 12 and 24 February in the 2017/18 summer period. The gridded sampling design with evenly distributed nodes at 10 m spacing was used for the probing, which was carried out at each of the grid nodes with a 1 cm diameter steel rod of 120 cm length. GPR data were collected along nine parallel profiles with north-south orientation, four profiles (Fig. 2) were selected for a
- 115 detailed analysis. GPR sounding was carried out using a shielded 500 MHz antenna and RAMAC CU-II control unit (MALÅ GeoScience, 2005). A wheel encoder was used to trig the measurements and control the distance along the profiles. The time window was set to 54.6 ns and scan spacing to 0.049 m. GPR data were processed using the REFLEXW software version 8.5 (Sandmeier, 2017). The depth axis of raw GPR profiles was converted from the time axis using the wave velocity determined from thaw depths probed at grid nodes and from the position of relevant reflector in GPR scans. The velocity obtained for
- 120 each sampling date ranged between 0.072 and 0.094 m ns⁻¹ increasing towards the late summer season with soil moisture (Fig. 3). The volumetric soil moisture was set as a mean value of 72 measurements recorded at each grid point of CALM-S JGM within 12 cm thick subsurface layer of the ground using the HydroSense II measuring device paired with the CS658 soil-water sensor (Campbell Scientific, Inc.).





125 **Figure 3 Relationship between mean surficial volumetric water content on CALM-S JGM and subsurface GPR wave velocities in active layer determined for the conversion of two-way travel times to depths.**

3.3 Snow cover observations

A long-term monitoring of snow depths is provided at 2-hour interval using the Judd (accuracy \pm 2 cm) ultrasonic sensor installed at the AWS-JGM. Raw readings from the sensor were corrected against actual air temperatures following the specification of the manufacturer (Judd Communication). Snow depth data are available for the summer season 2017/18 due to sensor failure prior to the summer 2016/17.

The extent of snow cover was identified using an unmanned aerial vehicle (UAV) imagery. DJI Phantom 3 Professional was used for the survey at a flight height of 30 m allowing the ground sample distance of approximately 1.0 cm. Pictures from the UAV were processed and orthorectified in Metashape (Agisoft) and used for the delimitation of snow patches in ArcMap 10.4 (ESRI) and interpolation of snow depth using the Radial Basis Function in Surfer 15 (Golden Software). The spatial distribution of snow depth was measured using GPR scanning and mechanical probing. The scanning with a shielded 800 MHz antenna was carried out along GPR profiles designed for ALT measurements and probing was done at each of the CALM-S grid nodes with a steel rod. The signal acquisition time of GPR scanning was set to 38.1 ns and scan spacing to 0.019 m. The probed snow depths were used to adjust the position of snow/ground interface in obtained GPR scans allowing for a precise conversion of time axis to depth.

4. Results:

4.1 Climate conditions in summer 2016/17 and 2017/18

Air temperature had a similar pattern in both seasons 2016/17 and 2017/18. Mean summer air temperature was between 0.1 °C (2016/17) and 0.0 °C (2017/18). Similarly, January air temperature ranged from 0.2 °C (2016/17) to -0.1 °C (2017/18). Daily temperatures mostly varied between 5.0 °C and -2.0 °C (Fig. 4). The warmest period occurred at the turn of January and February in both seasons). Summer TDD_A reached 83 °Cdays in 2016/17 and 67 °Cdays in 2017/18 (Table 1).

Mean seasonal ground temperatures on AWS-JGM ranged from 4.3 °C (2016/17) and 3.4 °C (2017/18) at a depth of 5 cm to -1.2 °C (2016/17) and -1.4 °C (2017/18) at a depth of 75 cm. Mean daily temperatures at a depth of 5 cm were mostly positive with the maximum values exceeding 10.0 °C in 2016/17 and 8.0 °C in 2017/18 (Fig. 4). Isothermal days at a depth of 5 cm occurred only twice in 2016/17, whereas 9 such days were observed in 2017/18 (Table 1). The summer TDD₅ were 398 °C days (2016/17) and 311 °C days (2017/18).



Table 1 Selected thermal characteristics of air temperature (AT) and ground temperature at a depth of 5 cm (GT₅) on AWS-JGM and AWS-CALM in the summer periods 2016/17 and 2017/18.

Season	Period	AT	TDD _A	AWS-JGM			AWS-CALM		
				GT ₅	TDD ₅	ITD*	GT ₅	TDD ₅	ITD*
2016/17	DJF	0.1	83	4.3	398	2	3.9	354	0
	January	0.2	26	4.0	117	0	3.5	101	0
2017/18	DJF	0.0	67	3.4	311	9	3.8	340	1
	January	-0.1	17	2.8	82	9	3.7	112	1

* ITD = isothermal days

Different pattern of mean seasonal ground temperatures was observed on AWS-CALM. While the temperature at a depth of 5 cm differed only slightly between 3.9 °C (2016/17) and 3.8 °C (2017/18), the differences in the depths of 50 and 75 cm were greater. Observed means were 1.5 °C (2016/17) and 0.9 °C (2017/18) at a depth of 50 cm and -0.1 °C (2016/17) and -0.7 °C (2017/18) at 75 cm. Mean daily temperatures at a depth of 5 cm only rarely dropped below 0 °C (Fig. 4). Their seasonal maximums exceeded 8.5 °C (2016/17) and 6.5 °C (2017/18). Only one isothermal day appeared in the season 2017/18. The summer TDD₅ were 354 °Cdays (2016/17) and 340 °Cdays (2017/18).

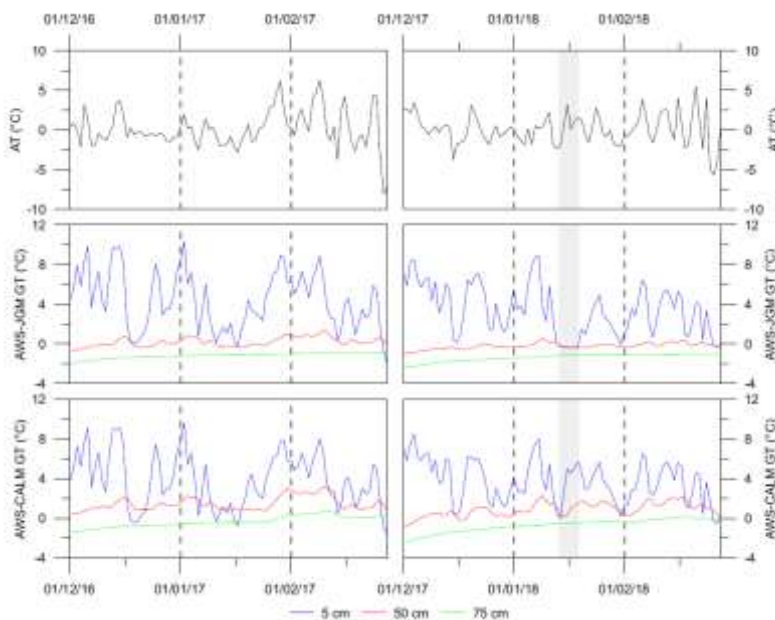


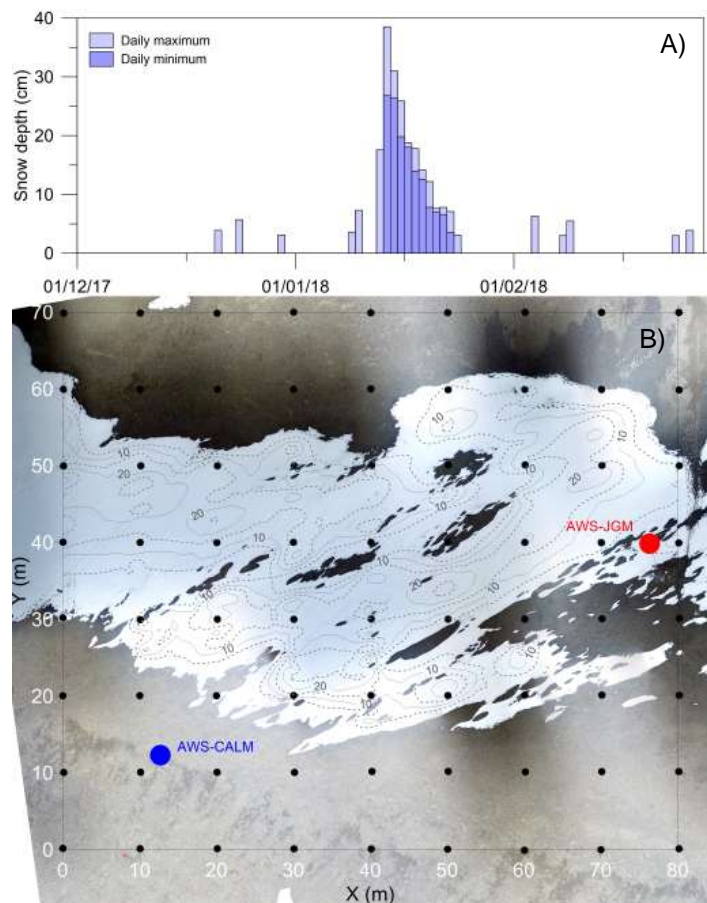
Figure 4 The variability of air temperature and ground temperatures at depths of 5, 50 and 75 cm on AWS-JGM and AWS-CALM in summer seasons 2016/17 and 2017/18. Grey rectangle indicates the period with compact snow cover detected on AWS-JGM.



4.2 Snow cover at CALM-S JGM site in January 2018

170 Snowstorm occurred between 13 January 22:00 UTC and 14 January 4:00 UTC. A relatively short period of 6 hr was sufficient to create snow cover that reached a maximum depth of 38 cm at AWS-JGM site. The most rapid thinning of the snowpack was observed on the 16 January when the snow depth decreased by 8 cm as a result of relatively high air temperatures that exceeded 6.0 °C in maximum. Snow persisted until 24 January when the last shallow snowpack (3 cm) melted (Fig. 5).

The distribution and thickness of snow were surveyed six days after the snowstorm, when snow cover extent was reduced to 46% of the CALM-S JGM area. The ground plan of the snow patch was complex and snow depth variable (Fig. 5) due to the redistribution by strong wind during the snowstorm and irregular melting after the storm. Snow drift produced irregular pattern of elongated zastrugi features and interleaving troughs with the SW-NE orientation. Owing to the drift, snow depth ranged from 20–30 cm on the ridges to less than 5 cm in troughs. While the maximum snow depths determined at probed profiles was 25 cm, the modelled mean snow depth was 10 cm. Within the snow patch, wind-blown ground appeared at seven places that increased rapidly in extent due to the enhanced snowmelt on the margins of bare ground.



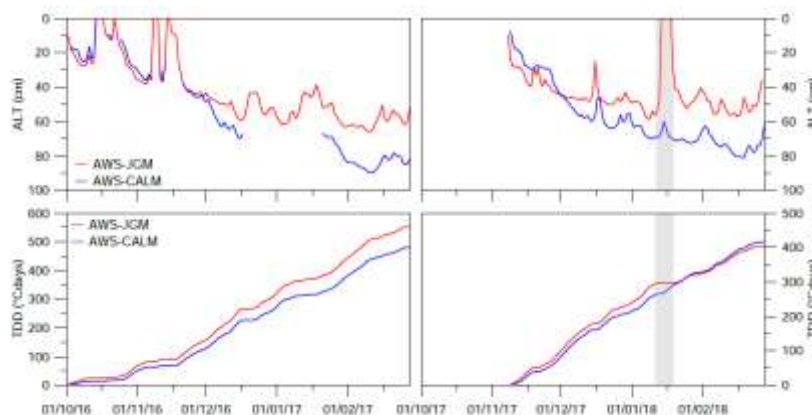
180



Figure 5 Variability of maximum daily snow depth on AWS-JGM in the summer 2017/18 (A). The distribution of snow with 10 cm isohyets of snow depth on CALM-S JGM on 20th January 2018 (B). Black points mark 10 m grid nodes, colour points represent the position of AWS-JGM (red) and AWS-CALM (blue).

185 4.3 Evolution of ALT during summer seasons 2016/17 and 2017/18

The active layer thawing in 2016/17 begun in early October, while it started around mid-November in 2017/18. The most rapid thawing propagation in the early thawing season at the turn of November and December was connected with a rapid increase in total TDD₅ during this period (Fig. 6). Thaw depths were around 50 cm (AWS-JGM) and 65 cm (AWS-CALM) in mid-December when the thawing propagation started to slow down (Fig. 6). The most pronounced interruption of thawing progress
190 was observed on AWS-JGM in January 2018 when the active layer refroze completely after a snowstorm. The maximum thicknesses on AWS-JGM reached 66 cm (10 February 2017) and 59 cm (8 January 2018). Observed maximums on AWS-CALM were 90 cm (11 February 2017) and 81 cm (18 February 2018). Total TDD₅ in thawing seasons reached 552 °C days (2016/17) and 404 °C days (2017/18) on AWS-JGM. The TDD₅ on AWS-CALM were 512 °C days (2016/17) and 416 °C days (2017/18).



195

Figure 6 Seasonal evolution of active layer thaw depth and thawing degree days (TDD₅) on AWS-JGM and AWS-CALM in the seasons 2016/17 and 2017/18. Dots indicate maximum thaw depths on both AWS sites. Grey rectangle indicates the period with compact snow cover detected on AWS-JGM.

The difference in ALT between the two subsequent summer seasons is clearly visible in Fig. 7 that also reveals relatively even
200 thaw plane during the summer 2016/17 and its irregular course in January 2018. The largest interannual difference in thaw depths coincides with those sections of the scanned profiles that were covered with thick continuous snowpack during the January 2018 measurement in profiles X20 and X40 (Fig. 7). Within these sections, the thaw plane is located 20 to 30 cm higher compared to the snow-free parts of the profiles. The thaw plane along the predominantly snow-free profile 70 in January



2018 is more or less parallel to the permafrost table observed in 2017 (Fig. 7). This is also the case of February measurements
205 in all measured profiles.

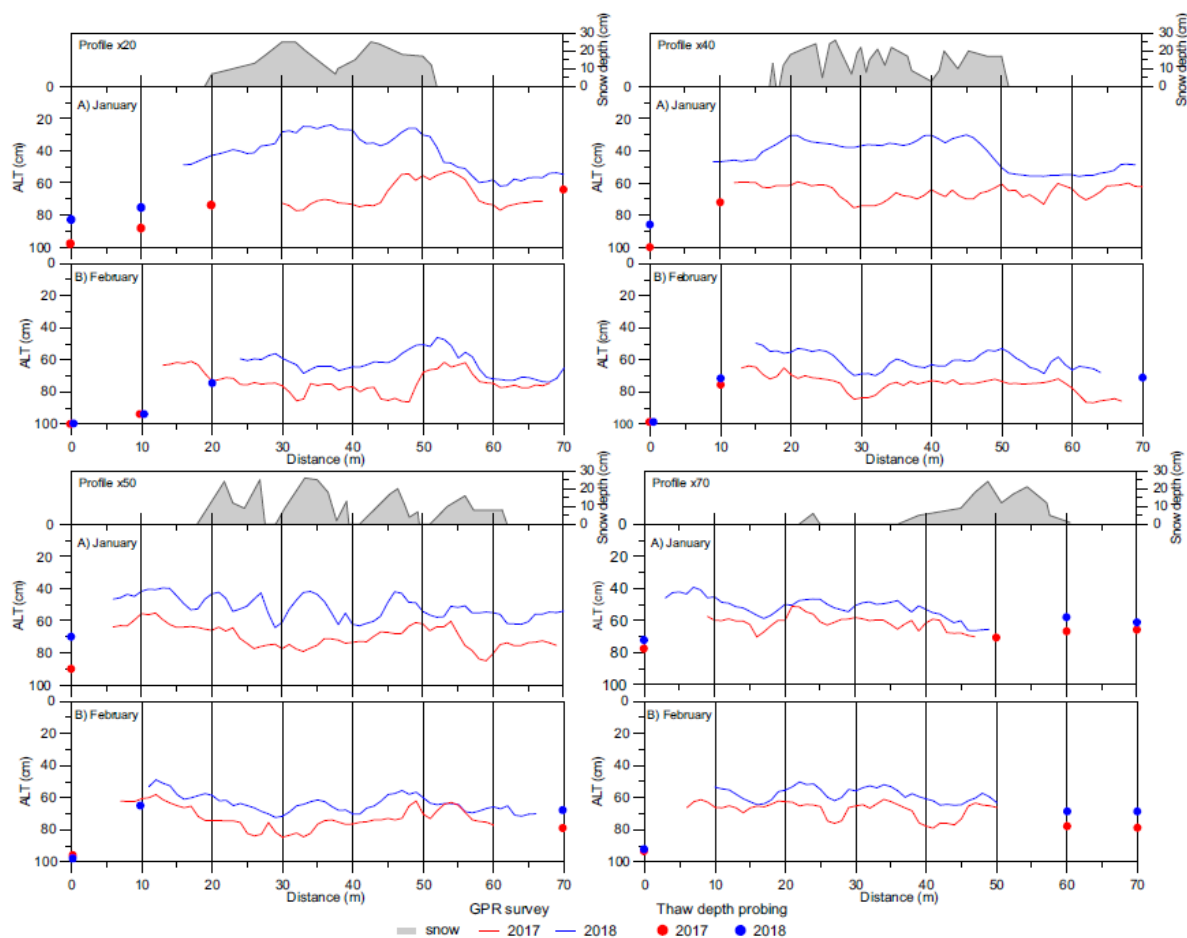
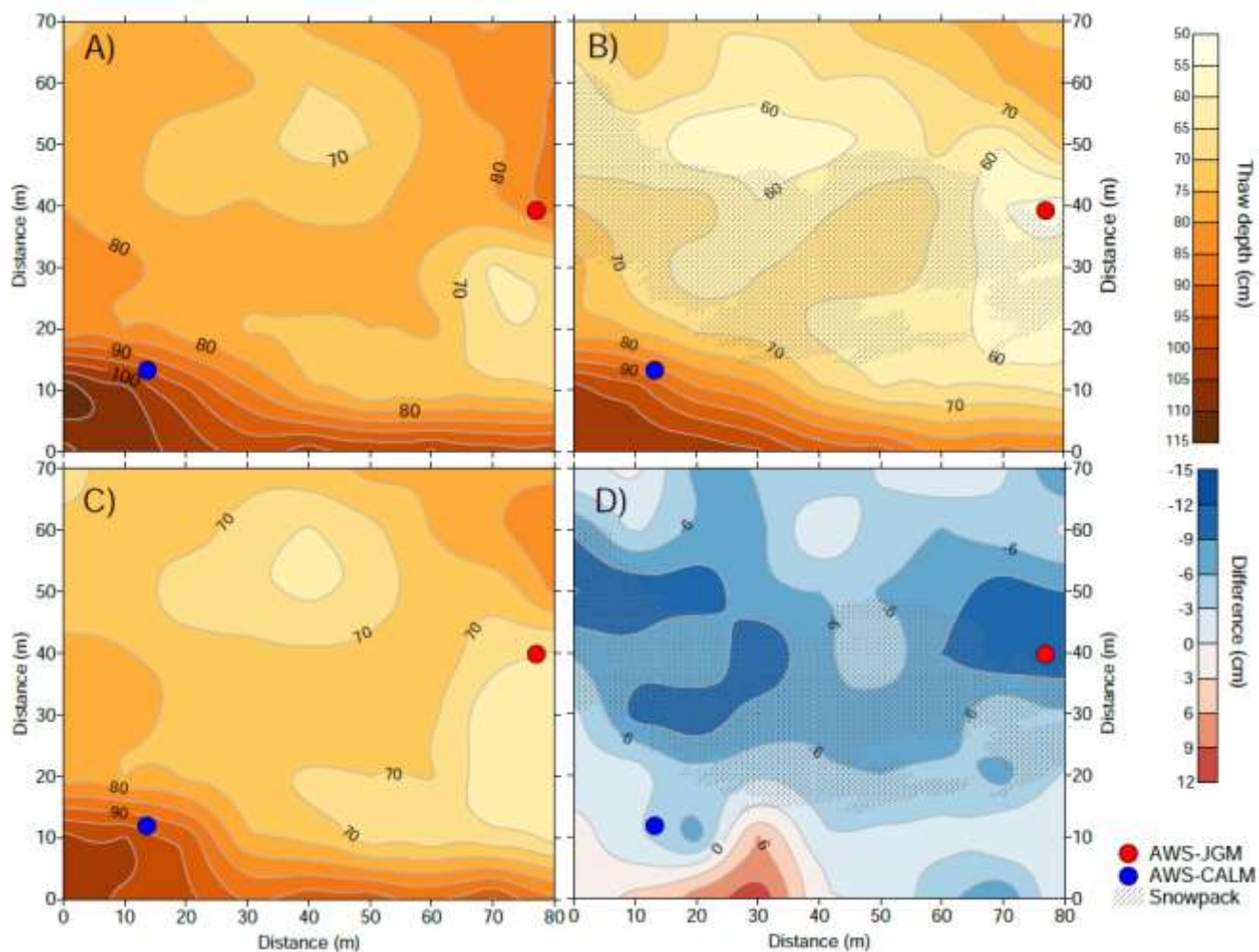


Figure 7 Snow cover depth (grey polygons) in January 2018 and thaw depths in January and February 2017 and 2018 determined from GPR measurements at CALM-S JGM site.

Spatial distribution of thaw depth for the CALM-S JGM site during the late summer 2016/17 and 2017/18 is illustrated in Fig.
210 8. Thaw depths were more spatially uniform in February 2017 although two geologically distinct parts of the study area are
clearly visible. The bimodal distribution with prevailing lower ALT (< 80 cm) and thaw depths as high as 115 cm along the
southern margin of the study area have already been observed over the years 2014–16. This large contrast in thaw depth has
been tentatively attributed to different grain size distribution and moisture content in two sedimentary units within the study
area (Hrbáček *et al.*, 2017). The strongly bimodal pattern can be seen in the 2018 grid that shows even more pronounced
215 difference in thaw depths between the two parts. The region of decreased ALT coincides with maximum snow depths in



January 2018 that is also consistent with the difference between mean thaw depths over the period 2014–17 and 2018 grid (Fig. 8D).



220 **Figure 8** Spatial variability of thaw depth on CALM-S JGM in A) February 2017, B) February 2018, C) mean thaw depth in the period 2014-2017 and D) difference between February 2018 and the 2014-2017 mean.

5. Interpretation and discussion

5.1 Climate conditions in the study area in the context of previous years

Air temperatures in the study area during the summer periods 2016/17 and 2017/18 were below long-term (2006–2015) summer average reported for the AWS-JGM and nearby Abernethy Flats sites (Hrbáček and Uxa, 2020). Even though mean
225 air temperature in the summer was the lowest in 2014/15, the year 2017/18 had the lowest TDD_A (Table 2) indicating a decrease in a total number of days with prevailing positive temperatures. The mean summer ground temperatures at a depth of 5 cm



were the lowest in the season 2017/18. Noticeable decrease of the mean seasonal ground temperatures was recorded primarily on AWS-JGM. In 2017/18, the mean summer ground temperature on AWS-CALM was higher than on AWS-JGM.

230 **Table 2** Variability of mean air temperatures and thawing degree days of air in AWS-JGM in the summer period 2014/15 and 2017/18.

Season	AT DJF (°C)	TDD _A (°Cdays)	DJF GT AWS-JGM (°C)	DJF GT AWS-CALM (°C)
2014/15*	-0.5	83	4.7	4.4
2015/16*	0.4	118	4.7	4.6
2016/17	0.1	83	4.3	3.9
2017/18	0.0	67	3.4	3.8

* data according to Hrbáček *et al.*, 2017.

235 Regardless of relatively cold summer ground surface temperatures, the thickest active layer and the highest TDD₅ on both AWS-JGM and AWS-CALM were observed in 2016/17 (Table 3). This was primarily caused by unusually warm spring months (September to November) in the north-eastern part of the AP (Turner *et al.*, 2020). Such conditions favoured early melting of the active layer in the beginning of October which started weeks earlier than usually (Hrbáček *et al.*, 2017; Hrbáček and Uxa, 2020). Sandy soil texture together with lower moisture also supports warmer surficial conditions on AWS-JGM as documented by TDD₅ increase by ca 28–50 °Cdays. However, TDD₅ were 12°C days lower in 2017/18 on AWS-JGM than on AWS-CALM.

240

Table 3 Variability of active layer thickness (ALT) and thawing degree days at a depth of 5 cm (TDD₅) and AWS-JGM and AWS-CALM in the period 2014/15–2017/18.

Season	ALT AWS-JGM (cm)	TDD ₅ AWS-JGM (°Cdays)	ALT AWS-CALM (cm)	TDD ₅ AWS-CALM (°Cdays)
2014/15*	63	456	86	418
2015/16*	65	506	87	478
2016/17	67	552	90	502
2017/18	59	404	82	416

* data according to Hrbáček *et al.*, 2017.

5.2 Snow cover effect on ground thermal regime

245 Variations in summer air temperature and the length of the thaw season control ALT but snow cover may reduce it significantly (e.g., Guglielmin, 2004; Zhang, 2005; Guglielmin *et al.*, 2012). While a cooling effect of thick long-lasting snow patches has been reported from different regions including AP (Guglielmin *et al.*, 2014b; Ramos *et al.*, 2017; 2020), the influence of thin snow cover that rapidly builds and melts during the warm period remains unknown. The ground thaw depths recorded in January 2018 at the CALM-S JGM site demonstrate a decrease in active layer thickness underneath ephemeral snow cover



250 with limited depth that protected the ground surface only for six days prior to ALT measurements. The initial maximum snow
depth of 38 cm falls within the range of 30–70 cm that is considered sufficient to isolate the ground from temperature variations
(e.g., de Pablo *et al.*, 2017; Kňázková *et al.*, 2020). However, the maximum snow depth of 25 cm observed on the CALM-S
JGM at the time of ALT measurements indicates much lower snow depth over most of the study area. Considering that ALT
thinning was observed far beyond the margin of the snowpack, a mean snow depth of 10 cm has sufficient influence on the
255 ground thermal regime. This value is significantly lower than the effective snow depth of 20 cm considered with respect to the
insulation effect of snow in AP region (de Pablo *et al.*, 2016; Oliva *et al.*, 2017a).

The largest impact of ephemeral snow cover on thaw depths in the study area can be seen underneath thick continuous
snowpack in profiles X20 and X40 (Fig. 7), where active layer thinning reaches 20 to 30 cm. By contrast, a slight overall
decrease (lower than 10 cm) in ALT was observed along profile X50 across irregularly thick snowpack with frequent holes
260 and at predominantly snow-free profile X70 (Fig. 7). The difference in thaw depths between snow-covered and bare surface
decreases rapidly after the snowmelt. The snow cover disappeared from the study area on 24 January and measurements from
12 February reveal the unimodal distribution of ALT. The rapid restoration of a more or less uniform thaw plane results from
the combination of relatively high air temperatures and an enhanced conduction of heat from the ground surface due to
meltwater percolation (*sensu* de Pablo *et al.*, 2014; Farzamian *et al.*, 2020). The influence of ephemeral snow cover on thaw
265 depths is apparent in the timing of the maximum ALT on snow-covered and bare sites. Whereas the maximum ALT on snow-
affected AWS-JGM site was observed before the snowstorm event on 9 January, the ALT maximum on a snow-free site
occurred on 18 February. The later culmination of the thaw depth at the snow-free site coincides well with the timing of the
maximum ALT in previous summer seasons which is typically around mid-February (Hrbáček *et al.*, 2017).

The ground temperatures recorded at the CALM-S JGM indicate that ephemeral snow cover may also affect thermal regime
270 of the active layer. As Fig. 4 shows, the presence of snow cover with an initial depth of 38 cm eliminates diurnal temperature
fluctuations down to a depth of 50 cm and results in a substantial decrease in the mean daily ground temperatures. The mean
monthly ground surface temperature in January is reduced by nearly one degree below the snow cover (with the depth
decreasing from 38 to 12 cm over six days) compared to the bare surface (Tables 1 and 2). Although the net cooling effect of
ephemeral snow over the summer season is limited, the number of isothermal days increases and TDD₅ are reduced by ca 10%
275 compared to snow-free summer seasons (Tables 1 and 3). This is in line with the reported insulating effect of snow patches
that persist over the warm season in permafrost conditions (de Pablo *et al.*, 2017). Guglielmin *et al.* (2014b) and Oliva *et al.*
(2017a) reported a cooling of the ground surface and a reduced magnitude of ground temperature fluctuations on Adelaide
Island, western AP; and Livingston Island, north-western AP, respectively. De Pablo *et al.* (2017) observed an increase in the
minimum ground surface temperatures below quasi-permanent snow patches on Livingston Island, north-western AP. The
280 observed changes in recorded ground temperatures confirm that the presence of snow cover may be more important for the
active layer refreezing and thaw plane position than summer temperatures (Zhang, 2005; de Pablo *et al.*, 2017; Ramos *et al.*,
2017).



5.3 Assessment of the results in a wider regional context of Arctic/mountain regions

285 The previous studies on JRI considered the winter snowpack as too thin and temporally unstable to create a sufficient insulation layer on the ground (Hrbáček *et al.*, 2016). This is mostly because of dynamic weather conditions during winter and prevailing strong southern winds which remove the snow from flat surfaces resulting in its irregular distribution within the terrain (Kavan *et al.*, 2020). In specific conditions of long-lasting snow accumulations, a snowpack more than 30 cm deep causes isothermal regime of ground temperature during the winter months (Kňázková *et al.*, 2020).

290 Most of the studies dealing with a relationships between snow and the ground thermal regime in Antarctica are located in the South Shetlands in the north-western AP. The oceanic climate makes this part of AP one of the wettest regions in Antarctica with precipitation rates of more than 1000 mm yr⁻¹ (Carrasco and Cordero, 2020). This results in high annual net snow accumulation and snow cover depth, with mean values of about 0.5 m (de Pablo *et al.*, 2017). Such snowpack can cause a significant warming of the ground compared to windswept areas (Oliva *et al.*, 2017a). As the northern AP is located in border conditions between continuous and discontinuous permafrost (Bockheim *et al.*, 2013; Obu *et al.*, 2020), regular and thick
295 snowpack in the winter months can lead to permafrost degradation (Hrbáček *et al.*, 2020). On the other hand, mean annual air temperature has decreased at a statistically significant rate since the beginning of the 20th century, with a most rapid cooling during the summer season (Turner *et al.*, 2016, Oliva *et al.*, 2017b). This was reflected in an increase in the number of snowfall events on the north-western side of the AP since the mid-2010s during the summer period (Carrasco and Cordero, 2020). Despite the fact that the trends in the annual total of precipitation from extreme precipitation events over 1979–2016 are small
300 (Turner *et al.*, 2019), positive trends in the precipitation total and summer snowfall events may result in a more frequent accumulation of ephemeral snow cover with a temporary cooling effect.

This study brings new insight into the functioning of the snow cover in relation to active layer thickness. So far, the active layer thinning was attributed mostly to long-lasting snow accumulation which prevented active layer thawing during the early warm season. Therefore, its thinning was directly related to the shortening of the thawing season (Ramos *et al.*, 2017; de Pablo
305 *et al.*, 2018). Consequently, the long-term active layer thinning rate was more likely connected with an increased duration of the snow cover, rather than with the climate variability during summer months (Ramos *et al.*, 2017). In other Antarctic regions, like Victoria Land, snowpack can persist for an entire summer and completely prevent active layer thawing (Guglielmin *et al.*, 2014a). However, the ephemeral snowpack's role in summer has not been reported yet from neither Antarctic nor Arctic regions. The influence of summer snowfalls and related snowpack on the thermal regime and thickness of the active layer has
310 been reported from alpine areas (Hanson and Hoelzle, 2004; Magnin *et al.*, 2017; Zhao *et al.*, 2018), but snow and ground conditions in the mountains differ strongly from those in high latitudes (Hoelzle and Gruber, 2008). Usually, the period of high summer is characterized by a low snowfall intensity and predominantly snow-free ground surface. Therefore, snowfall events leading to an accumulation of more than 30 cm deep snow cover are scarce.



6. Conclusions

315 This study brings a new perspective on the effect of snow cover on active layer thermal regime and thickness in the Antarctic Peninsula region. The recent research deals mostly with the role of winter or permanent snow cover, whereas the role of ephemeral snow occurring during the high summer was not documented at all in Antarctica. This study shows that even short-term presence of a relatively thick snow cover during the high summer can significantly affect active layer thermal regime and thawing propagation. Considering the observations from 2017/18 within the context of the snow-free seasons with similar air
320 temperature conditions, the ephemeral snow cover considerably affected the ground thermal regime and active layer thickness. The magnitude of the snow insulation effect was controlled by the snow depth and duration of snowpack. The observed snowpack with an initial snow depth of 38 cm lasted for 12 days during the high summer season. Below the ephemeral snow cover, the diurnal temperature fluctuations were limited down to a depth of 50 cm, thaw depths decreased by nearly 20%, the maximum active layer thickness was observed almost six weeks prior to the maximum on a snow-free site, and the mean
325 monthly ground temperature was reduced by nearly one degree compared to the snow-free surface. The number of isothermal days increased and TDD₅ were reduced by ca 10% in the presence of snow cover.

Data availability

All data are available upon request to FH.

Author contribution:

330 FH and ZH designed the research hypothesis, wrote the manuscript and participated in fieldwork. MK and JS participated in fieldwork.

Competing interests

The authors declare that they have no conflict of interest.

Acknowledgement:

335 The research was supported by the Ministry of Education, Youth and Sports of the Czech Republic projects LM2015078 and CZ.02.1.01/0.0/0.0/16_013/0001708; by the Masaryk University project MUNI/A/1356/2019; and by the Czech Science Foundation project GC20-20240S. The authors acknowledge the crew of JGM station, particularly Jakub Ondruch for providing UAV imagery and Kamil Laska for the support on the meteorological measurements setting and maintenance.



References

- 340 Bockheim, J., Vieira, G., Ramos, M., López-Martínez, J., Serrano, E., Guglielmin, M., Wilhelm, K. and Nieuwendam, A.: Climate warming and permafrost dynamics in the Antarctic Peninsula region, *Glob. Planet. Change*, 100, 215–223. doi:10.1016/j.gloplacha.2012.10.018, 2013.
- Callaghan, T. V., Johansson, M., Brown, R. D., Groisman, P. Y., Labba, N., Radionov, V., Bradley, R. S., Blangy, S., Bulygina, O. N., Christensen, T. R., Colman, J. E., Essery, R. L. H., Forbes, B. C., Forchhammer, M. C., Golubev, V. N., Honrath, R.
- 345 E., Juday, G. P., Meshcherskaya, A. V., Phoenix, G. K., Pomeroy, J., Rautio, A., Robinson, D. A., Schmidt, N. M., Serreze, M. C., Shevchenko, V. P., Shiklomanov, A. I., Shmakin, A. B., Skořd, P., Sturm, M., Woo, M. K. and Wood, E. F.: Multiple effects of changes in arctic snow cover, *Ambio*, 40, 32–45 doi:10.1007/s13280-011-0213-x, 2011.
- Campbell, B., Claridge, G. G. C., Campbell, D. I. and Balks, M. R.: OF THE MCMURDO DRY VALLEYS , ANTARCTICA The soils in the McMurdo Dry Valley region are a key component, *Am. Geophys. Union*, 1998.
- 350 Carrasco, J. F. and Cordero, R. R.: Analyzing Precipitation Changes in the Northern Tip of the Antarctic Peninsula during the 1970–2019 Period, *Atmosphere (Basel)*, 11(12), 1270. doi:10.3390/atmos11121270, 2020.
- de Pablo, M.A., Ramos, M., Molina, A., Vieira, G., Hidalgo, M. A., Prieto, M., Jiménez, J. J., Fernández, S., Recondo, C., Calleja, J. F., Peón, J. J. and Mora, C.: Frozen ground and snow cover monitoring in the South Shetland Islands, Antarctica: Instrumentation, effects on ground thermal behaviour and future research. *Cuad. Investig. Geográfica*, 42, 475–495.
- 355 <https://doi.org/10.18172/cig.2917>, 2016.
- de Pablo, M.A., Ramos, M. and Molina, A.: Snow cover evolution, on 2009-2014, at the limnopolare lake CALM-S site on Byers peninsula, Livingston island, Antarctica. *Catena*, 149, 538–547. <https://doi.org/10.1016/j.catena.2016.06.002>, 2017
- Farzamian, M., Vieira, G., Monteiro Santos, F. A., Yaghoobi Tabar, B., Hauck, C., Catarina Paz, M., Bernardo, I., Ramos, M. and Angel De Pablo, M.: Detailed detection of active layer freeze-thaw dynamics using quasi-continuous electrical resistivity tomography (Deception Island, Antarctica), *Cryosphere*, 14, 1105–1120. doi:10.5194/tc-14-1105-2020, 2020.
- 360 Goodrich, L. E.: The influence of snow cover on the ground thermal regime., *Can. Geotech. J.*, 19, 421–432. doi:10.1139/t82-047, 1982.
- Guglielmin, M.: Observations on permafrost ground thermal regimes from Antarctica and the Italian Alps, and their relevance to global climate change, *Glob. Planet. Change*, 40(1–2), 159–167. [https://doi.org/10.1016/S0921-8181\(03\)00106-1](https://doi.org/10.1016/S0921-8181(03)00106-1),
- 365 2004.
- Guglielmin, M.: Ground surface temperature (GST), active layer and permafrost monitoring in continental Antarctica, *Permafr. Periglac. Process.*, 17, 133 – 143. doi:10.1002/ppp.553, 2006.
- Guglielmin, M., Worland, M. R. and Cannone, N.: Spatial and temporal variability of ground surface temperature and active layer thickness at the margin of maritime Antarctica, Signy Island, *Geomorphology*, 155, 20–33,
- 370 doi:10.1016/j.geomorph.2011.12.016, 2012.



- Guglielmin, M., Dalle Fratte, M. and Cannone, N.: Permafrost warming and vegetation changes in continental Antarctica, *Environ. Res. Lett.*, 9(4), 045001, doi:10.1088/1748-9326/9/4/045001, 2014a.
- Guglielmin, M., Worland, M. R., Baio, F. and Convey, P.: Permafrost and snow monitoring at Rothera Point (Adelaide Island, Maritime Antarctica): Implications for rock weathering in cryotic conditions, *Geomorphology*, 225, 47–56, doi:10.1016/j.geomorph.2014.03.051, 2014b.
- Hanson, S. and Hoelzle, M.: The thermal regime of the active layer at the Murtèl rock glacier based on data from 2002, *Permafr. Periglac. Process.*, 15, 273–282, doi:10.1002/ppp.499, 2004.
- Harris, C., Arenson, L. U., Christiansen, H. H., Etzelmüller, B., Frauenfelder, R., Gruber, S., Haeberli, W., Hauck, C., Hölzle, M., Humlum, O., Isaksen, K., Kääb, A., Kern-Lütschg, M. A., Lehning, M., Matsuoka, N., Murton, J. B., Nötzli, J., Phillips, M., Ross, N., Seppälä, M., Springman, S. M. and Vonder Mühl, D.: Permafrost and climate in Europe: Monitoring and modelling thermal, geomorphological and geotechnical responses, *Earth-Science Rev.*, 92(3), 117–171, doi:10.1016/j.earscirev.2008.12.002, 2009.
- Harris, S. A. and Corte, A. E.: Interactions and relations between mountain permafrost, glaciers, snow and water, *Permafr. Periglac. Process.*, 3(2), 103–110, doi:10.1002/ppp.3430030207, 1992.
- Hoelzle, M. and Gruber, S.: Borehole and ground surface temperatures and their relationship to meteorological conditions in the Swiss Alps. In: Kane, D.L. and Hinkel, K.M. (Eds.): *9th International Conference on Permafrost*, 29 June –03 July 2008, Fairbanks, Alaska. Fairbanks: Institute of Northern Engineering. pp. 723–728. <https://doi.org/10.5167/uzh-2825>, 2008.
- Hrbáček, F., Kňázková, M., Nývlt, D., Láska, K., Mueller, C.W. and Ondruch, J.: Active layer monitoring at CALM-S site near J.G. Mendel station, James Ross Island, eastern Antarctic Peninsula. *Sci. Total. Environ.*, 601–602, 987–997. doi:10.1016/j.scitotenv.2017.05.266, 2017.
- Hrbáček, F., Láska, K. and Engel, Z.: Effect of snow cover on the active-layer thermal regime – a case study from James Ross Island, Antarctic Peninsula. *Permafr. Periglac. Processes.*, 27(3), 307–315. <https://doi.org/10.1002/ppp.1871>, 2016.
- Hrbáček, F., Nývlt, D., Láska, K., Kňázková, M., Kampová, B., Engel, Z., Oliva, M. and Mueller, C.W.: Permafrost and active layer research on James Ross Island: An overview. *Czech Polar Reports*, 9(1), 20–36. <https://doi.org/10.5817/CPR2019-1-3>, 2019.
- Hrbáček, F., Oliva, M., Fernández, J.-R., Kňázková, M. and de Pablo, M.A.: Modelling ground thermal regime in bordering (dis)continuous permafrost environments. *Environ. Res.*, 181, 108901. <https://doi.org/10.1016/j.envres.2019.108901>, 2020.
- Hrbáček, F. and Uxa, T.: The Evolution of a Near-Surface Ground Thermal Regime and Modelled Active-Layer Thickness on James Ross Island, Eastern Antarctic Peninsula, in 2006–2016. *Permafr. Periglac. Processes.*, 31, 141–155. doi:10.1002/ppp.2018, 2020.
- Johansson, M., Callaghan, T. V., Bosiö, J., Åkerman, J., Jackowicz-Korczynski, M. and Christensen, T.: Rapid responses of permafrost and vegetation to experimentally increased snow cover in sub-arctic Sweden. *Environ. Res. Lett.*, 8(3), 035025. <https://doi.org/10.1088/1748-9326/8/3/035025>, 2013.



- Judd Communications: *Judd Communications Depth Sensor.* Available at:
405 <http://static1.1.sqspcdn.com/static/f/1146254/15414722/1322862508567/ds2manual.pdf>. [Accessed 31 January 2020], 2011.
- Kavan, J., Nývlt, D., Láska, K., Engel, Z. and Kňázková, M.: High-latitude dust deposition in snow on the glaciers of James Ross Island, Antarctica. *Earth Surf. Process. Landf.*, 45, 1569–1578. <https://doi.org/10.1002/esp.4831>, 2020.
- Kňázková, M., Hrbáček, F., Kavan, J. and Nývlt, D.: Effect of hyaloclastite breccia boulders on meso-scale periglacial-aeolian landsystem in semi-arid antarctic environment, james ross island, antarctic peninsula, *Geogr. Res. Lett.*, 46, 7–31,
410 [doi:10.18172/cig.3800](https://doi.org/10.18172/cig.3800), 2020.
- Magnin, F., Westermann, S., Pogliotti, P., Ravel, L., Deline, P. and Malet, E.: Snow control on active layer thickness in steep alpine rock walls (Aiguille du Midi, 3842ma.s.l., Mont Blanc massif). *Catena*, 149(2), 648–662. <https://doi.org/10.1016/j.catena.2016.06.006>, 2017.
- MALÅ GeoScience.: *Ramac GPR. Hardware manual*. Malå: MALÅ GeoScience., 2005.
- 415 Obu, J., Westermann, S., Vieira, G., Abramov, A., Balks, M.R., Bartsch, A., Hrbáček, F., Kääb, A. and Ramos, M.: Pan-Antarctic map of near-surface permafrost temperatures at 1 km² scale. *Cryosphere*, 14, 497–519. <https://doi.org/10.5194/tc-14-497-2020>, 2020.
- Oliva, M., Hrbáček, F., Ruiz-Fernández, J., de Pablo, M.Á., Vieira, G., Ramos, M. and Antoniadis, D.: Active layer dynamics in three topographically distinct lake catchments in Byers Peninsula (Livingston Island, Antarctica). *Catena*, 149, 548–559.
420 <https://doi.org/10.1016/j.catena.2016.07.011>, 2017a.
- Oliva, M., Navarro, F., Hrbáček, F., Hernández, A., Nývlt, D., Perreira, P., Ruiz-Fernández, J., Trigo, R.: Recent regional climate cooling on the Antarctic Peninsula and associated impacts on the cryosphere. *Sci. Total. Environ.*, 580, 210–223. <http://dx.doi.org/10.1016/j.scitotenv.2016.12.030>, 2017b.
- Palerme, C., Genthon, C., Claud, C., Kay, J.E., Wood, N.B. and L'Ecuyer, T.: Evaluation of current and projected Antarctic precipitation in CMIP5 models. *Clim. Dyn.*, 48(1–2), 225–239. <https://doi.org/10.1007/s00382-016-3071-1>, 2017.
- 425 Park, H., Walsh, J., Fedorov, A.N., Sherstikov, A.B., Iijima, Y. and Ohata, T.: The influence of climate and hydrological variables on opposite anomaly in active-layer thickness between Eurasian and North American watersheds. *Cryosphere*, 7, 631–645. <https://doi.org/10.5194/tc-7-631-2013>, 2013.
- Ramos, M., Vieira, G., de Pablo, M.A., Molina, A., Abramov, A. and Goyanes, G.: Recent shallowing of the thaw depth at
430 Crater Lake, Deception Island, Antarctica (2006–2014). *Catena*, 149(2), 519–528. <https://doi.org/10.1016/j.catena.2016.07.019>, 2017.
- Ramos, M., Vieira, G., de Pablo, M.A., Molina, A. and Jimenez, J.J.: Transition from a Subaerial to a Subnival Permafrost Temperature Regime Following Increased Snow Cover (Livingston Island, Maritime Antarctic). *Atmosphere*, 11, 1332. <https://doi.org/10.3390/atmos11121332>, 2020.
- 435 Sandmeier, K.J.: Reflexw: processing program for seismic, acoustic and electromagnetic reflection, refraction and transmission data, version 8.5. Karlsruhe: Sandmeier Scientific Software, 2017.



- Turner, J., Lu, H., White, I., King, J.C., Phillips, T., Hosking, J.S., Bracegirdle, T.J., Marshall, G.J., Mulvaney, R. and Deb, P.: Absence of 21st century warming on Antarctic Peninsula consistent with natural variability. *Nature*, 535, 411–415. <https://doi.org/10.1038/nature18645>, 2016.
- 440 Turner, J., Phillips, T., Thamban, M., Rahaman, W., Marshall, G.J., Wille, J. D., Favier, V., Winton, V.H.L., Thomas, E., Wang, Z., van den Broeke, M., Hosking, J.S. and Lachlan-Cope, T.: The dominant role of extreme precipitation events in Antarctic snowfall variability. *Geophys. Res. Lett.*, 46, 3502–3511. <https://doi.org/10.1029/2018GL081517>, 2019.
- Turner, J., Marshall, G., Clem, K., Colwell, S., Phillips, T. and Lu, H.: Antarctic temperature variability and change from station data. *Int. J. Climatol.*, 40 (6), 2986 – 3007. <https://doi.org/10.1002/joc.6378>, 2020.
- 445 van Wessem, J.M., Ligtenberg, S.R.M., Reijmer, C.H., van de Berg, W.J., van den Broeke, M.R., Barrand, N.E., Thomas, E.R., Turner, J., Wuite, J., Scambos, T.A. and van Meijgaard, E.: The modelled surface mass balance of the Antarctic Peninsula at 5.5 km horizontal resolution. *Cryosphere*, 10, 271–285. <https://doi.org/10.5194/tc-10-271-2016>, 2016.
- Zhang, T.: Influence of the seasonal snow cover on the ground thermal regime: An overview, *Rev. Geophys.*, 43, RG4002 doi:10.1029/2004RG000157, 2005.
- 450 Zhao, J.Y., Chen, J., Wu, Q.B. and Hou, X.: Snow cover influences the thermal regime of active layer in Urumqi River Source, Tianshan Mountains, China. *Journal of Mountain Science*, 15(12), 2622–2636. <https://doi.org/10.1007/s11629-018-4856-y>, 2018.